HBRC Journal (2013) 9, 216–226

Housing and Building National Research Center

HBRC Journal

http://ees.elsevier.com/hbrcj

Behavior of post-tensioned fiber concrete beams

Hossam-eldin Abd-elazim Elsharkawy [a], Tamer Elafandy [b,*], Abdel Wahab EL-Ghandour [b], Amr Ali Abdelrahman [b]

[a] *Dept. of Structural Engineering, Ain Shams University, Cairo, Egypt*
[b] *Dept. Housing and Building National Research Center, Giza, Egypt*

Received 3 June 2012; accepted 21 June 2012

KEYWORDS

Partially prestressed;
Fully prestressed;
T-shaped;
Steel fibers;
Polypropylene fibers;
Cracks-width;
Flexural strength;
Ductility;
Energy absorption

Abstract This paper presents an experimental and analytical study on the behavior of post-tensioned concrete beams with variable discontinuous fibers' content. Eleven half scale T-shaped post-tensioned simple beams were cast and tested in four points bending under the effect of a repeated load using a displacement control system up to failure. The test parameters were the fibers' type (steel and polypropylene) and content, as well as the prestressing ratio (partially or fully). Key test results showed considerable enhancement in the crack distribution, crack width and spacing, concrete tensile strength and flexural stiffness in all beams with steel fibrous concrete. The latter aspects were directly proportional to the steel fibers' contents. On the other hand, beams containing polypropylene fibers demonstrated a slight decrease in the flexural strength and a slight increase in flexural stiffness. In addition, the tensile steel strains decreased in all fibrous concrete beams, with lowest values in steel fibrous concrete specimens when compared to those of the polypropylene fibers. Furthermore, fibrous concrete beams also demonstrated enhanced ductility and energy absorption, which reached the highest values for steel fibrous concrete specimens. Generally, it can be concluded that steel fibers proved to have higher structural efficiency than polypropylene fibers, when used in the tested specimens.

Introduction

Prestressed concrete has emerged very quickly as the predominant material in use in the construction industry, but the concrete has low tensile strength and low ductility. Over the past 10 years, there has been a steady increase in the use of fiber reinforced concrete (FRC) to help overcome the low tensile strength and ductility of concrete. The fibers were added to control the cracking of reinforced concrete, and to alter the behavior of the material once the concrete has cracked by bridging the cracks and, hence, providing post-cracking ductility. Recently, the building code requirements for structural concrete (ACI 318-08) [1] mentioned steel fiber in two chapters (material-shear & torsion). The available research in the area of post-tensioned prestressed beams using concrete containing fibers (3–10) is very sparse. Accordingly, necessary research has to be done in order to evaluate the effect of fibers on the

* Corresponding author.
E-mail addresses: hosharkawy@yahoo.com (H.-e.A.-e. Elsharkawy), tamer_elafandy@yahoo.com (T. Elafandy).

Peer review under responsibility of Housing and Building National Research Center.

ELSEVIER Production and hosting by Elsevier

1687-4048 © 2013 Housing and Building National Research Center. Production and hosting by Elsevier B.V. All rights reserved.
http://dx.doi.org/10.1016/j.hbrcj.2013.08.006

behavior of post-tensioned prestressed beams from ductility and serviceability perspectives.

This paper presents an experimental investigation in the behavior of post-tensioned fibrous concrete beams when tested under repeated load using the displacement control system up to failure. The fibers contents' ratios, type of fibers (steel and polypropylene) as well as the prestressing level (partially or fully) were the main parameters investigated. The test results including capacity, crack patterns, deflection, and tensile steel strain in the flexural reinforcement are presented and discussed. Key structural aspects of behavior including ductility and energy absorption are also discussed. In addition, a previously proposed analytical model [3] was used to predict the test results. The validation of the model was established through comparisons with tests. Finally, design oriented conclusions are highlighted.

Experimental work

Beam details

Figs. 1 and 2 show the geometry, supports arrangement, internal reinforcement and prestressing profile of all tested specimens, which consisted of eleven half scale post-tensioned simple beams with typically T-shaped cross-section and equal spans. All beams had the same overall dimensions with a total length of 5400 mm, an overall height of 300 mm and a clear span of 5000 mm. The dimensions of the flange were 350 mm × 60 mm and the web dimensions were 240 mm × 150 mm, as shown in the figures. All beams were designed according to ACI 318-08 [1] to have the same ultimate moment capacity. The prestressing profiles were kept the same for all beams. The web stirrups in all beams were consisting of 2 vertical branches of 10 mm diameter bars that were horizontally spaced at 100 mm, in order to prevent shear failure occurrence prior to the flexural failure. In addition, the transverse reinforcement of the flanges consisted of 8 mm diameter bars spaced at 200 mm. All the prestressing strands comprised of seven wires with a nominal diameter of 12.7 mm and 15.24 mm for partially prestressed and fully prestressed beams, respectively. The beams were divided into three groups according to the partial prestressing ratio (PPR) and the types of fibers. Group one comprised four specimens coded B1-FP-0-0, B2-FP-0.5-S, B3-FP-1-S and B4-FP-1.5-S, and reinforced with prestressing strands only in order to simulate the full prestressing system (PPR = 1). In the previous beams, the steel fibers' contents were 0, 0.5%, 1%, and 1.5% of the concrete volume respectively. Group two consisted of four specimens reinforced with prestressing strands and flexural reinforcement, in order to simulate the partial prestressing (PPR = 0.73) system. The specimens of this group were coded B5-PP-0-0, B6-PP-0.5-S, B7-PP-1-S and B8-PP-1.5-S with steel fibers' contents of 0%, 0.5%, 1% and 1.5% of the concrete volume, respectively. Finally, group three consisted of three specimens reinforced with prestressing strands and flexural reinforcement similar to the second group, but with polypropylene fibers' contents of 0.5%, 1%, and 1.5% of the concrete volume. Beams coded B1-FP-0-0 and B5-PP-0-0 without fibers were used as control beams for the fully prestressed (PPR = 1) and the partially prestressed (PPR = 0.73) conditions, respectively.

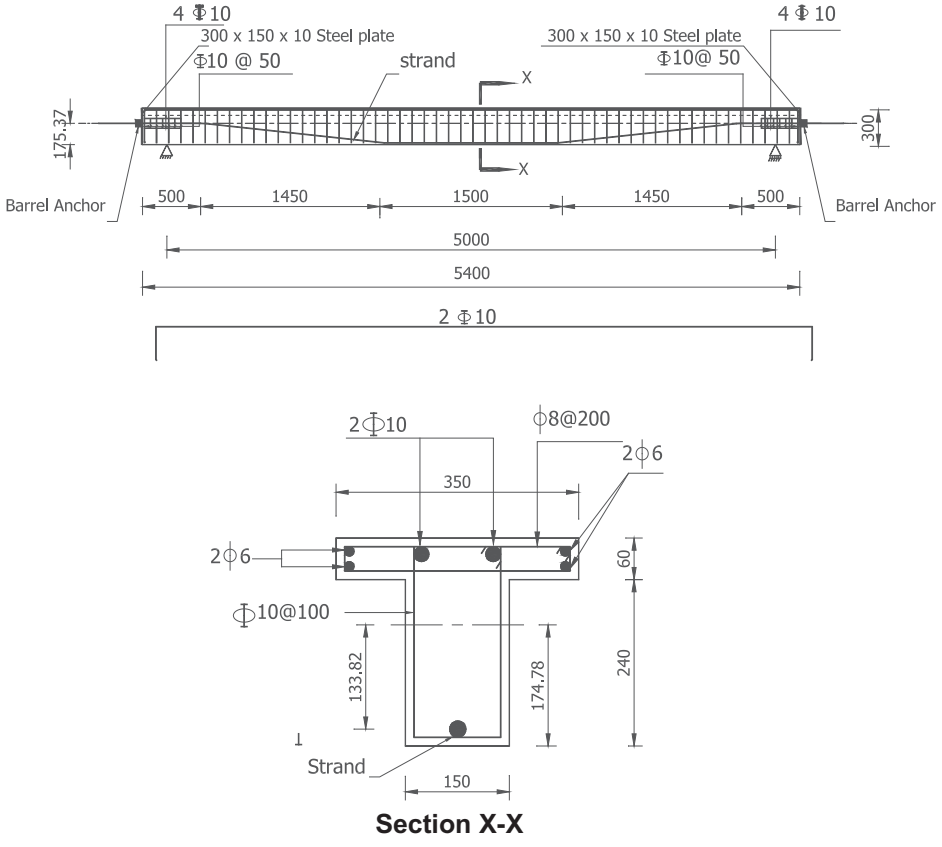

Fig. 1 Flexural reinforcement for fully prestressed beams of group one. Typical details for fully prestressed beams of group one.

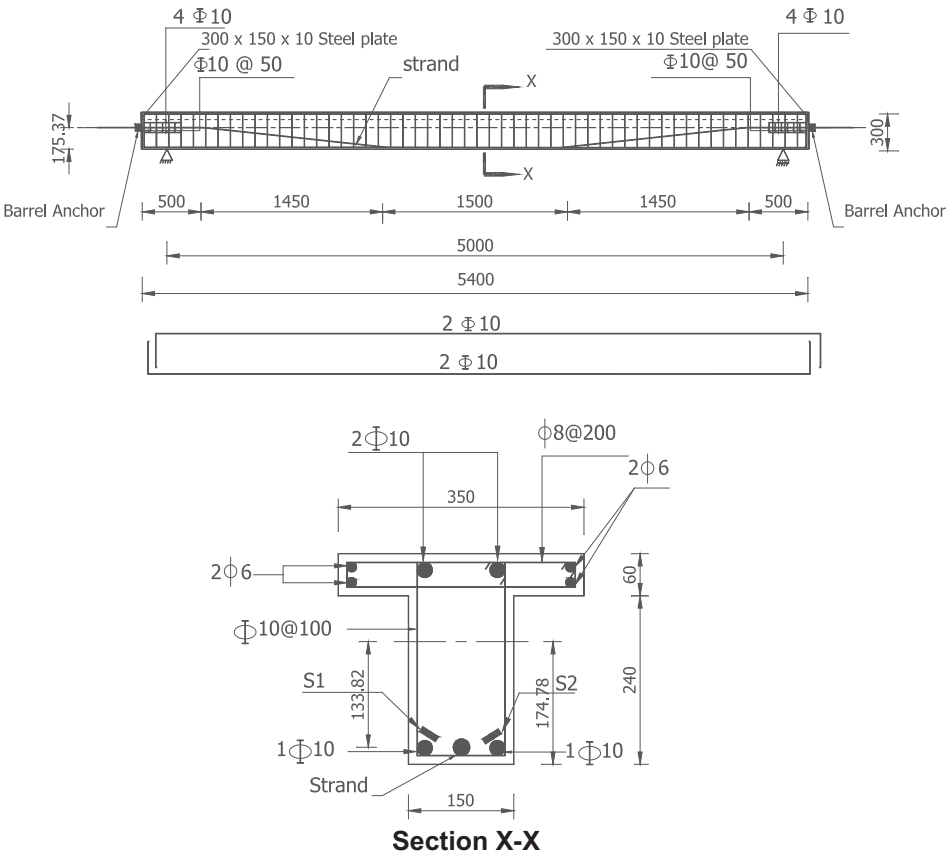

Fig. 2 Flexural reinforcement for partially prestressed beams of groups two and three. Typical details for partially prestressed beams of groups two and three.

Material properties

Deformed high grade steel (400/600) bars of 10 mm diameter, with yield stress f_y = 470 N/mm^2 and ultimate tensile strength f_u = 700 N/mm^2 were used as main longitudinal reinforcement and stirrups. The transverse reinforcement used for the flanges was made of mild steel (240/350) bars of 6 mm and 8 mm diameter, respectively, with yield stress f_y = 240 N/mm^2 and ultimate tensile strength f_u = 350 N/mm^2. All steel reinforcement had a constant modulus of elasticity, E_s = 200 kN/mm^2.

The prestressing strands were made of high grade steel strands comprising seven individual wires each. The strands had diameters of 15.24 mm and 12.7 mm which were tested in the lab demonstrating ultimate tensile strengths of 1990 MPa and 1730 MPa, respectively. The latter value (1730 MPa) did not match the manufacturer's testing report, due to some problems in the anchorage system of the machine. Therefore, the ultimate tensile strength was taken as 1860 MPa for design.

The target compressive strength for concrete was f'_c = 32 MPa after 28 days. The concrete used was a normal weight concrete with mix proportions of 4.45 kN/m^3 ordinary Portland cement, 6.86 kN/m^3 sand from natural resources, 12.54 kN/m^3 crushed limestone and a water cement ratio of 0.44. Sikament-163 M was used to improve the workability of concrete with a dosage of 2% of the weight of the cement.

Two kinds of discontinuous fibers were added to the concrete mix; namely, polypropylene and steel. The polypropylene fibers (Propex) were of variable lengths from 12 mm to 18 mm and their specific gravity was 0.91, while the mild carbon steel fibers of crimped shape were of average length of 55 mm, average thickness of 0.44 mm, width of 2.1 mm and with aspect ratio of 50.7 (length to equivalent diameter). Finally, grout (Addi-grout) with specific gravity of 0.64 was used to be injected through the corrugated plastic ducts.

Casting and prestressing process

Eleven plywood forms were prepared for casting the concrete. All forms had the same dimensions. The steel reinforcement cages were prepared and put into the forms. Corrugated plastic ducts for strands were accurately and symmetrically installed about mid-span in the forms. Two end-bearing plates were positioned at the two ends of all beams to distribute the prestressing force over all the cross sections of the beams in order to avoid any cracks in the anchorage zone.

The discontinuous polypropylene or steel fibers were added by chopping during concrete mixing. The concrete was compacted for two minutes after casting, using an electrical poker vibrator, followed by water curing and covering with polythene sheeting for one week. For control purposes, 48 cylinders with 150 mm diameter and 300 mm height, were cast alongside the specimens from the same concrete batch and were cured with the specimens. The cylinders were tested before prestressing and at the same day of testing the beams. Table 1 shows the summary of the beams' details and compressive concrete strength.

Table 1 Summary of beams details and compressive strength of concrete.

Group	Specimen	Volume of fibers (%)	Type of fibers	Partial prestressing ratio (PPR)	Compressive strength f'_c (MPa) at testing day
One	B1-FP[a]-0[e]-0	0	-	1	43.15
	B2-FP-0.5[f]-S[c]	0.5	Steel	1	43.5
	B3-FP-1[g]-S	1	Steel	1	44.2
	B4-FP-1.5[h]-S	1.5	Steelw	1	44.9
Two	B5-PP[b]-0-0	0	-	0.73	43.15
	B6-PP-0.5-S	0.5	Steel	0.73	43.5
	B7-PP-1-S	1	Steel	0.73	44.2
	B8-PP-1.5-S	1.5	Steel	0.73	44.9
Three	B9-PP-0.5-P[d]	0.5	Polypropylene	0.73	43
	B10-PP-1-P	1	Polypropylene	0.73	39.9
	B11-PP-1.5-P	1.5	Polypropylene	0.73	38.2

[a] FP = fully prestressed.
[b] PP = partially prestressed.
[c] *S* = steel fibers.
[d] *P* = polypropylene fibers.
[e] 0 = Without fiber.
[f] 0.5 = Volume of the fibers equal 0.5% of the concrete volume.
[g] 1 = Volume of the fibers equal 1% of the concrete volume.
[h] 1.5 = Volume of the fibers equal 1.5% of the concrete volume.

After two months from casting of the concrete, the prestressing force was applied at 75% of the ultimate strength of the strands for both 12.7 mm and 15.24 mm diameters. One mono barrel anchor was installed at each end of the beams since all beams had two live ends. A hydraulic jack that was calibrated at the lab of the Housing and Building National Research Center was used in the prestressing process. The stressing forces were transferred from the hydraulic jack to the strands along four equal stages ranging from 25% to 100% of the required force. The force in the strands was measured using a donut load cell. In addition, the elongation of the strands was measured at every stressing stage. Grouting started as soon as the strands were stressed using a special pump for grout injection. The grout was injected under pressure into the duct inlet until it came out from the duct outlet. The beams were left for one week until the grout gained its strength according to the instructions of the manufacturing company.

Instrumentation

The crack propagation was monitored and crack width was measured at all levels of loading using a microscope having an accuracy of 0.1 mm. In addition, Linear Variable Distance Transducers (LVDTs) with 0.01 mm accuracy were used to measure the mid-span deflections of all beams, as shown in Fig. 3. The strains in the non-prestressed steel were measured in the longitudinal direction as previously indicated (S1 and S2) in Fig. 2. Finally, the data were collected using a data acquisition system and "lab view" software at a rate of 1 sample per two seconds.

Test setup and loading procedure

Fig. 3 shows the details of the test set-up. It should be noted that the test arrangement was symmetrical about the mid-span section of all beams. Each beam was loaded in four loading points bending. The beams were subjected to a cyclic loading up to failure, using a hydraulic machine of 500 kN capacity. The load was applied on the beams using a stroke control system, which divided the machine load that was applied through a steel spreader beam 1.5 m in length, as shown in the figure. The cyclic loading was achieved by increasing the stroke with 2.5 mm increments up to 15 mm and 5 mm increments up to 50 mm, and finally with 10 mm increments until failure, as shown in Fig. 4.

Discussion of test results

Crack patterns, failure mode and crack width

Figs. 5–7 show the crack patterns at failure of all tested beams. On the other hand, Fig. 8 shows the total load versus the average cracks width and Table 2 shows the value of cracking load and range of spacing between the cracks of all the tested beams.

For all beams, the crack propagation followed similar traditional flexural patterns in simple beams and the first tension cracks appeared in the constant moment zone. In addition, the tested beams experienced two distinct modes of failure. In the fact, beams of group one with PPR = 1 (fully prestressed) failed in compression due to crushing of concrete in the compression zone followed by cutting of the strands. On the other hand, beams of groups two and three with PPR = 0.73 (partially prestressed) experienced conventional ductile flexural failure due to yielding of the main bottom steel followed by concrete crushing.

For all beams, crack propagation followed the similar traditional flexural patterns in simple beams and the first tension cracks appeared in the constant moment zone. In addition, the tested beams experienced two distinct modes of failure. In fact, beams of group one with PPR = 1 (fully prestressed) failed in compression due to the crushing of concrete in the compression zone followed by cutting of the strands. On the other

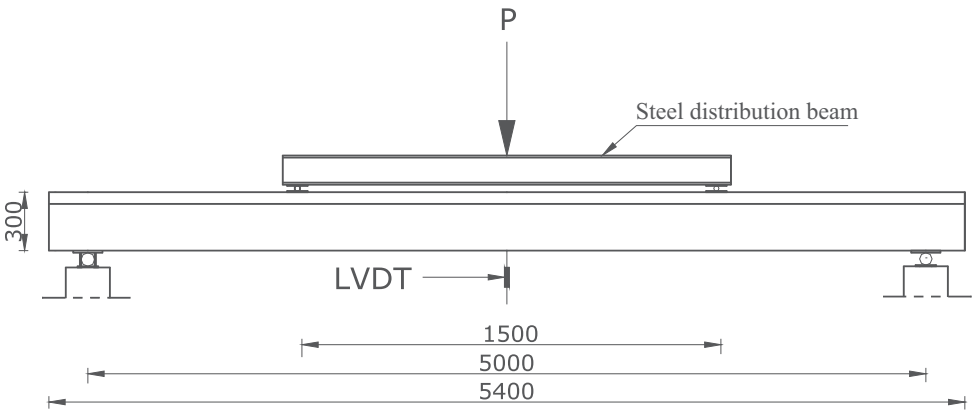

Fig. 3 Instrumentation and test setup of all specimens.

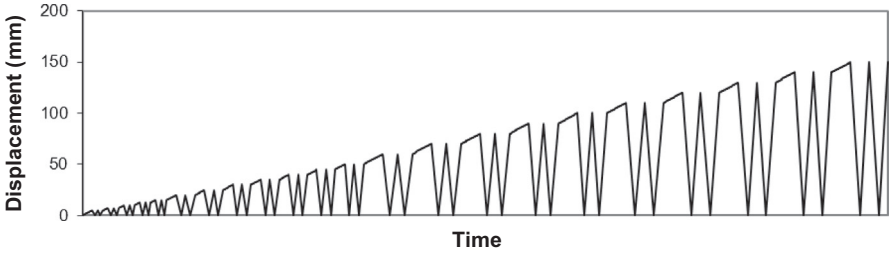

Fig. 4 Cyclic loading pattern for the specimens.

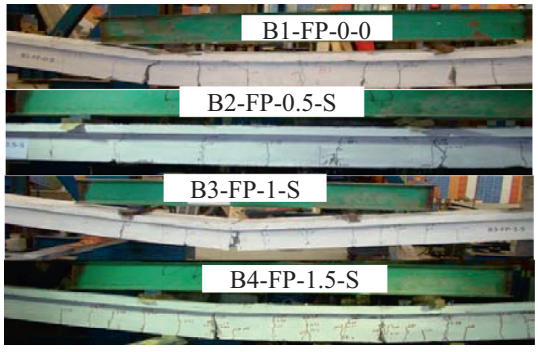

Fig. 5 Crack pattern on failure of beams in group one.

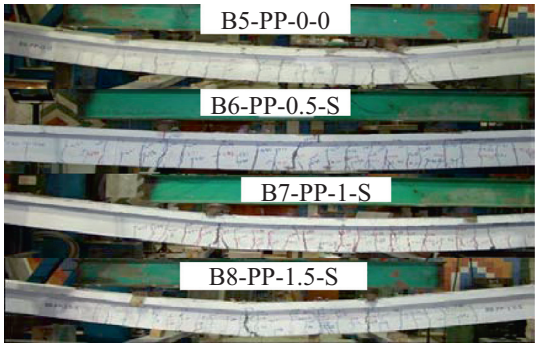

Fig. 6 Crack pattern on failure of beams in group two.

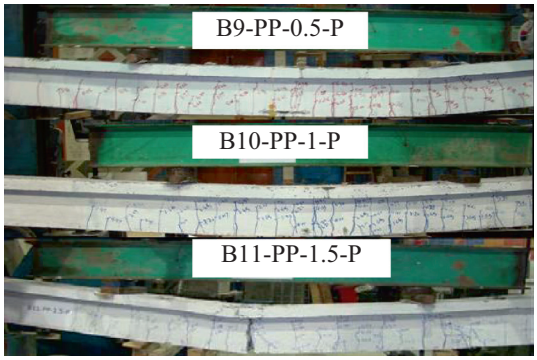

Fig. 7 Failure crack pattern of beams in group three.

hand, beams of groups two and three with PPR = 0.73 (partially prestressed) experienced conventional ductile flexural failure due to yielding of the main bottom steel followed by concrete crushing.

For all beams containing steel fibers of groups one and two (PPR = 1, PPR = 0.73), it can be noted that increasing the amount of steel fibers results in increased cracking loads and decreased the cracks' spacing and widths when compared to the respective control specimens. This is attributed to the increased cracks' numbers, hence, resulting in a more uniform crack propagation covering longer portions of the beams' spans when compared to the respective control specimens.

Table 2 shows that for all the partially prestressed beams of group three with PPR = 0.73, the cracking loads were slightly less than the corresponding control beam B5-PP-0-0 and decreased by increasing the polypropylene fibers' content unlike

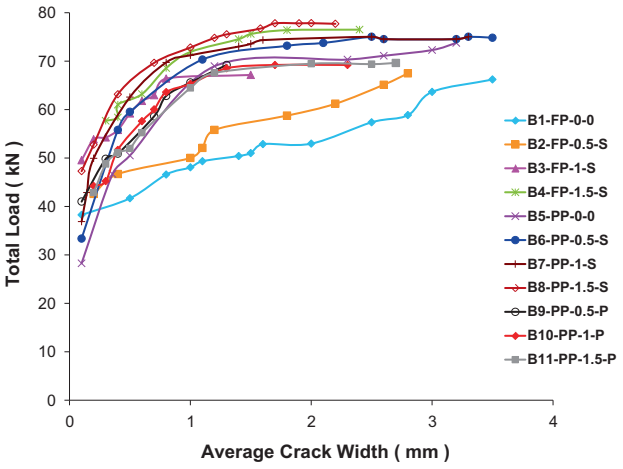

Fig. 8 Total applied load versus average crack width.

the beams with steel fibers. Fig. 8 also shows that the pre-maximum load average cracks' widths of these beams were slightly lower than their control specimen. Nonetheless, after the peak load, the average cracks' widths became bigger than their control beam, as shown in the same figure. Generally, it can be noted that the cracks' propagation were more uniform, in terms of higher cracks' numbers at decreased spacing and covering a longer portion of the beams' spans, when compared to the corresponding control beam, as shown in Fig. 7.

From the previous discussion, the higher efficiency of steel fibers when compared to polypropylene fibers, in increasing the flexural rigidity and in arresting the growth of cracks can be noted. This may be attributed to the poor bond of polypropylene with concrete as well as the low modulus of elasticity of polypropylene when compared to steel fibers. In addition, all the latter aspects were directly proportional to the fibers' contents. Finally, it can be noted that neither the inclusion of fibers nor the increase of its content in concrete changed the failure mode.

Ductility and energy absorption

Table 3 shows the ductility indices, increase in ductility, energy absorption and increase in energy absorption for all the tested beams. The deflection ductility index represented by Naaman et al. [2] was used to calculate the ductility indices for all tested beams. In this respect, the previous measure was defined as follows [2]:

$$\mu = \frac{1}{2}\left(\frac{E_{tot}}{E_{el}} + 1\right)$$

where E_{tot} is the total energy, which is equal the inelastic energy E_{in} plus the elastic energy E_{el}. Enhancement of ductility was calculated as the difference between the ductility index of the fibrous beam and the ductility index of the corresponding control beam divided by the ductility index of the corresponding control beam. The energy absorption was represented by the area up to failure under the curve of the total applied load versus mid-span deflection.

It can be noted that the ductility indices, enhancement of ductility indices, energy absorption and enhancement in energy absorption for all tested beams, containing steel fibers and polypropylene fibers were higher than the respective control ones, as shown in Table 3. In addition, the ductility indices, enhancement in ductility indices and energy absorption for partially prestressed (PPR = 0.73) beams of group two containing steel fibers were higher than the fully prestressed beams (PPR = 1) of group one containing similar amount of steel fibers as well as the partially prestressed beams of group three containing similar amount of polypropylene fibers. The table also shows that the enhancement ductility indices, energy absorption and enhancement in energy absorption for beams containing polypropylene fibers demonstrated lowest values when compared to their respective beams of group one (fully prestressed) and group two (partially prestressed) containing steel fibers. Furthermore, the table shows that beam B8-P-1.5-S with PPR = 0.73 demonstrated highest ductility index and enhancement in ductility index (3.67% and 33.37% respectively), when compared to all other beams containing steel or polypropylene fibers. On the other hand, beam B4-FP-1.5-S with PPR = 1 demonstrated highest enhancement (45.18%) in energy absorption, while B8-PP-1.5-S demonstrated the highest value of energy absorption, when compared to all tested beams.

Generally, the table shows that the increase in ductility indices and energy absorption was normally proportional to

Table 2 Cracking loads, peak load and spacing between cracks.

Group	Beam	Cracking load (kN)	Percentage of increase in cracking load (%)	Peak load (kN)	Percentage of increase in peak load (%)	Percentage of spacing between cracks load (mm)
One	B1-FP-0-0	38.3	–	67.28	–	280–320
	B2-FP-0.5-S	39.3	2.6	69.83	3.78	270–290
	B3-FP-1-S	47.6	24.28	72.2	7.3	230–250
	B4-FP-1.5-S	49.7	29.7	75	11.48	190–210
Two	B5-PP-0-0	25.7	–	71.85	–	126–147
	B6-PP-0.5-S	26.9	4.67	73.56	2.38	108–115
	B7-PP-1-S	29.8	16	74.8	4.11	95–100
	B8-PP-1.5-S	33.2	29.5	77.82	8.32	85–97
Three	B9-PP-0.5-P	24.6	−4.2	70.7	−1.5	100–110
	B10-PP-1-P	21.6	−15.9	70.94	−1.3	95–100
	B11-PP-1.5-P	20.2	−21.4	70.48	−1.9	93–99

Table 3 Ductility indices and energy absorption of all the tested beams.

Group	Beam	*E* (inelastic) (kN mm)	*E* (elastic) (kN mm)	*E* (total) (kN mm) energy absorption	Ductility index	Increase of ductility index (%)	Increase of energy absorption (%)
One	B1-FP-0-0	5545.04	3384.77	8929.8	1.82	–	–
	B2-FP-0.5-S	6370.38	3351.12	9721.51	1.95	7.2	8.86
	B3-FP-1-S	7555.36	3385.99	10941.35	2.12	16.77	22.52
	B4-FP-1.5-S	9357.02	3608.15	12965.17	2.29	26.22	45.18
Two	B5-PP-0-0	8316.7	2208.85	10525.55	2.88	–	–
	B6-PP-0.5-S	9861.25	2173.31	12034.56	3.27	13.39	14.33
	B7-PP-1-S	10753.33	2156.86	12910.19	3.49	21.16	22.65
	B8-PP-1.5-S	11831.05	2207.89	14038.94	3.68	27.63	33.37
Three	B9-PP-0.5-P	8749.76	2136.72	1088.46	3.05	5.7	3.4
	B10-PP-1-P	9322.26	2184.43	11506.7	3.13	8.7	9.32
	B11-PP-1.5-P	9743.88	2029.76	11773.64	3.4	17.9	11.85

the increase in fibers' content. The previous results also confirmed the higher efficiency of steel fibers in increasing the ductility and energy absorption when compared to those of the polypropylene fibers.

Effect of steel fibers percentage on the behavior of fully prestressed beams (PPR = 1)

Table 2 shows the peak load and the percentage enhancement of the peak load for all tested beams. The percentage enhancement of the peak load for the fibrous beam was calculated as the difference between their peak loads and that of their corresponding control beam, divided by the peak load of the corresponding control beam.

The table shows that the peak loads of all fibrous concrete beams of group one with PPR = 1 and contained steel fibers were higher than the corresponding control beam B1-FP-0-0. Beam B4-FP-1.5-S also demonstrated the highest peak load of 75 kN and percentage enhancement of 11.48%, when compared to all the beams of group one containing steel fibers.

Fig. 9 shows the total applied load versus mid-span deflection responses for beams of group one. The figure shows that all beams exhibited similar pre-cracking stiffness and deflection responses. In addition, all beams containing steel fibers exhibited higher post-cracking stiffness responses and lower deflections when compared to the corresponding control beam at similar load levels. This is mainly due to the higher tensile strength and better post-cracking behavior of fibrous concrete, which resulted in higher tension stiffening for the beams with fibrous concrete. The tension stiffening resulted in higher internal couple and less curvature of the cross section of the beams. The previous results confirm the high efficiency of steel fibers in increasing all aspects of structural behavior in terms of cracks widths, cracks propagation, flexural stiffness, and deflection. Finally, all the latter aspects were directly proportional to the steel fibers' content.

Effect of steel fibers percentage on the behavior of partially prestressed beams (PPR = 0.73)

The peak load group of two beams with PPR = 0.73 and containing steel fibers was higher than the corresponding control beam B5-PP-0-0, as shown in Table 2. In addition, beam B8-PP-1.5-S demonstrated the highest values for peak load

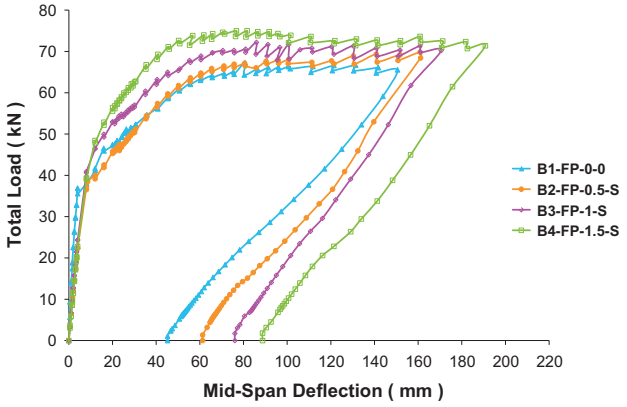

Fig. 9 Total applied load versus mid-span deflection for fully prestressed beams of group one.

(77.82 kN) and percentage of peak load enhancement (8.32%) when compared to all the other beams of group two. Similar to the fully prestressed specimens, the previous clearly shows the peak load increases by increasing the steel fibers' content.

Fig. 10 shows the total applied load versus mid-span deflection responses for beams of group two. A similar pre and post-cracking behavior to that of the fully prestressed beams is observed.

Fig. 11 shows the total applied load versus the tensile steel strain of the flexural steel bars at the mid-span sections of all partially prestressed beams. It can be noted from the figure that all beams had similar pre-cracking responses. Furthermore, all the reinforcing bars of fibrous beams yielded a higher load than the corresponding control beam B5-FP-0-0. This is mainly due to the higher tensile strength and better post-cracking behavior of fibrous concrete which resulted in higher tension stiffening for the beams with fibrous concrete. In addition, the beam B8-PP-1.5-S demonstrated the highest yielding load of all beams in group two. Furthermore, the figure shows that the tensile steel strains decreased by increasing the steel fibers' contents when compared at the same load levels. This result confirms the stiffer post-cracking response for all beams containing steel fibers. All the latter aspects were also directly proportional to the steel fibers' contents, as shown in Fig. 11.

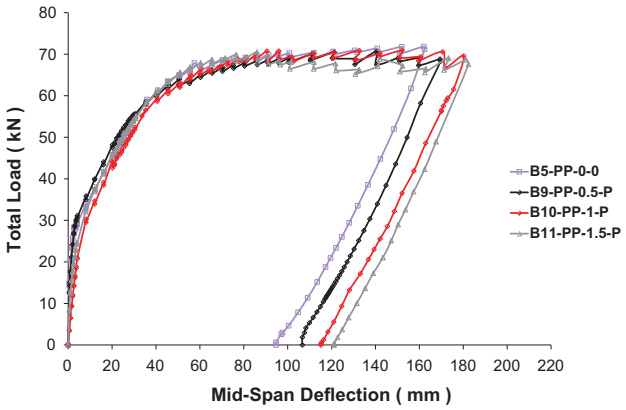

Fig. 10 Total applied load versus mid-span deflection for partially prestressed beams of group two.

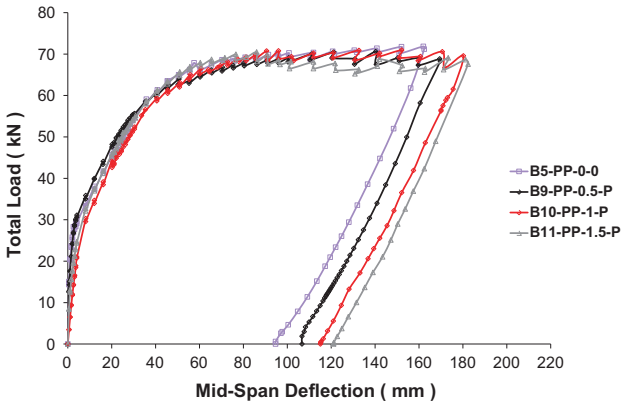

Fig. 12 Total applied load versus mid-span deflection for partially prestressed beams of group three.

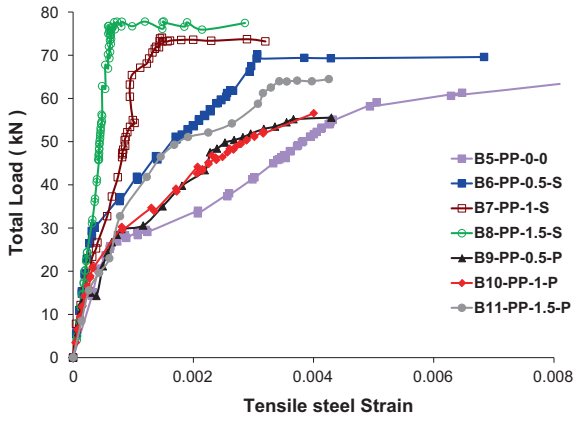

Fig. 11 Total applied load versus tensile steel strain of the flexural reinforcement at the mid-span.

Effect of polypropylene fibers percentage on the behavior of partially prestressed beams (PPR = 0.73)

Table 2 shows that the peak load and the percentage enhancement of peak load (−1.5%, −1.3%, and −1.9% for beams B9-PP-0.5-P, B10-PP-1-P and B11-PP-1.5-P, respectively) for all beams containing polypropylene fibers (group three) were slightly lower than those of the corresponding control beam B5-PP-0-0.

Fig. 12 shows the total applied load versus mid-span deflection responses of group three beams and their control specimen. It can be noted that the deflection of beams containing polypropylene fibers was nearly equal or slightly higher than the corresponding control beam at same load levels, until peak load of these beams. After the peak load, the figure shows that the beams of group three exhibited similar stiffness and deflection compared to the corresponding control beam at the same load levels.

From Fig. 11, it can be noted that beams containing polypropylene fibers showed a slight increase in the yielding loads when compared to the corresponding control beam B5-PP-0-0. The figure also shows that the tensile steel strain of the former beams was slightly higher than the corresponding control beam at same load levels. The post-cracking behavior of two beams with 0.5% and 1% of polypropylene fibers was similar, while increasing the polypropylene fibers content to 1.5% resulted in better serviceability in terms of less steel strains. This may be attributed to the higher tension stiffening of the beams containing fibers where the bond between polypropylene fibers and concrete at low load level was good. With the increase of the applied load, the bond between the polypropylene fibers and concrete becomes less and therefore it has no effect on the ultimate capacity of the beams.

Comparison between the effect of varying the steel fibers' content on the fully and partially prestressing beams

Table 2 shows that the peak load (71.85 kN) of the control beam B5-PP-0-0 of groups two and three with PPR = 0.73 was higher than that of the control beam of group one (67.28 kN) with PPR = 1. In addition, the table shows that all beams containing steel fibers demonstrated increased peak loads when compared to the respective control ones. Furthermore, the table shows that beam B8-PP-1.5-S with PPR = 0.73 (group two) had the highest peak load (77.82 kN) when compared to all other beams with PPR = 0.73 and PPR = 1 containing steel fibers. On the other hand, beam B4-FP-1.5-S (group one) with PPR = 1 showed the highest percentage of increased peak load (11.48%).

Fig. 13 shows the total applied load versus mid-span deflection responses for all beams of groups one and two containing steel fibers. The figure shows that all beams exhibited similar pre-cracking stiffness and deflection responses. In addition, the control beam B5-PP-0-0 with PPR = 0.73 (partially prestressed) exhibited higher post-cracking stiffness response and smaller deflection when compared to the control beam B1-FP-0-0 with PPR = 1 (fully prestressed) at the same load levels. Furthermore, all beams containing steel fibers exhibited higher post-cracking stiffness responses and smaller deflections when compared to their respective control ones at same load levels. The figure also shows that, at same load levels, group two beams with PPR = 0.73 (partially prestressed) exhibited higher post-cracking stiffness and lower deflections when compared to their respective group one beams with PPR = 1 (fully prestressed) containing similar steel fibers' content. In fact, it can be noted that beam B6-PP-0.5-S with PPR = 0.73 and

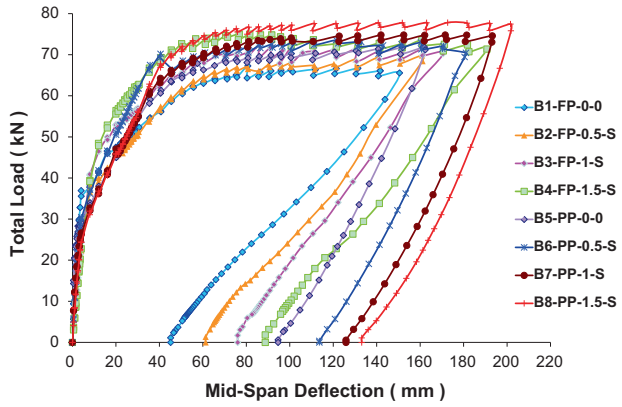

Fig. 13 Total applied load versus mid-span deflection for fully and partially prestressed beams of groups one and two.

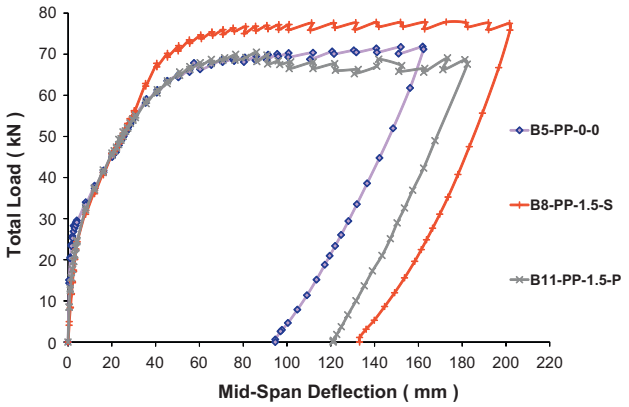

Fig. 14 Total applied load versus mid-span deflection for partially prestressed beams, B5-PP-0-0, B8-PP-1.5-S and B11-PP-1.5-P.

containing 0.5% steel fibers showed nearly similar post-cracking stiffness and deflection response to beam B4-FP-1.5-S with PPR = 1 and containing 1.5% steel fibers at same load levels. In addition, the figure shows that beam B8-PP-1.5-S with PPR = 0.73 and containing 1.5% steel fibers experienced the highest post-cracking stiffness and lowest deflection response when compared to the other beams with either PPR = 0.73 or PPR = 1 at same load levels. All the previous aspects were directly proportional to the steel fibers' content, as shown in the figure. The previous generally shows the higher efficiency of steel fibers in increasing the stiffness and decreasing the deflections.

Effect of type of fibers on the behavior of partially prestressed beams (PPR = 0.73)

Table 2 shows test results of beams of groups two and three with PPR = 0.73, and containing steel and polypropylene fibers, it can be noted that the peak load of the beams containing steel fibers were higher than the corresponding beams containing polypropylene fibers with similar content. In addition, the table shows that the peak load of the control beam of groups two and three (B5-PP-0-0) was higher than those of all beams containing polypropylene fibers. Furthermore, Table 2 shows that beam B8-PP-1.5-S demonstrated the highest peak load (77.82 kN) when compared to all beams of groups two and three.

Fig. 14 shows the total for beams B5-PP-0-0, B8-PP-1.5-S and B11-PP-1.5-P as representative of the effect of type of fibers on the behavior of beams with PPR = 0.73. The figure shows that all tested beams exhibited similar pre-cracking stiffness and deflection responses. The figure also shows the stiffer deflection response of beam B8-PP-1.5-S containing steel fibers, where lower deflection was monitored when compared to the corresponding control beam B5-PP-0-0 and beam B11-PP-1.5-P containing polypropylene fibers. This obviously shows the higher efficiency of steel fibers in increasing the stiffness and decreasing the deflections when compared to the polypropylene fibers. The yielding load of beam B8-PP-1.5-S containing steel fibers was also higher than the corresponding control beam B5-PP-0-0 and beam B11-PP-1.5-P containing polypropylene fibers, as shown in Fig. 11. In addition, Fig. 11 shows that the tensile steel strains of beam B8-PP-1.5-S was lower than the corresponding control beam B5-PP-0-0 and beam B11-PP-1.5-P containing polypropylene fibers, at the same load levels. All the previous results clearly confirm the higher structural efficiency of steel fibers than the polypropylene fibers.

Analytical analysis

Analytical model

The analytical model proposed by Swamy et al. [3] was used in this research to predict the ultimate load of all the steel fibrous concrete beams (partially and fully prestressed beams). An analytical study was not conducted for the beams containing the polypropylene fibers since there was no consensus on the results of beams containing polypropylene fibers in the previous researches.

Fig. 15 shows the stress strain diagram of the model used in this research. A simple modification was done on the compression stress block from a serpentine curve to a rectangular block [3]. The conventional compatibility and equilibrium condition for the normal reinforced concrete was used in this model. The analysis of the compression block was based on the ACI 318-08 [1]. The tensile contribution of steel fibers was represented by the trapezoidal stress block shown in Fig. 15. The peak tensile stress of the fibrous concrete σ_m, was at a distance z from the extreme compression fibers, as shown in the figure.

Fig. 15 shows that the value of the tensile strength of fibrous reinforced concrete beams, σ_{cu}, at the bottom of the section is:

$$\sigma_{cu} = \tau_o \tau_l \tau_b 2\tau \frac{l_f}{d_f} \rho \quad (1)$$

where τ_o is the orientation factor, τ_l is the length correction factor, τ_b is the bond efficiency factor, τ is the interfacial bond stress between the fibers and the matrix, l_f is the length of fibers, d_f is the diameter of fibers, and ρ is the fibers' volume percent by volume of the total concrete mixture.

The previous Eq. (1) contained three correction factors; namely, the orientation factor, τ_o, that was taken as 0.41(11) due to the fact that a portion of fibers was inefficiently oriented. The length correction factor, τ_l, to account for the stress distribution at the end portion of the fibers, is as follows:

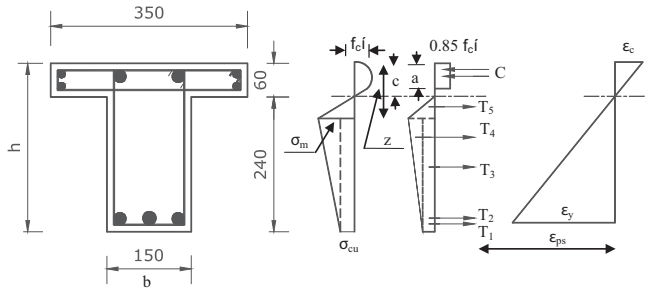

Fig. 15 Stress and strain diagram for the analytical model.

$$\tau_i = 1 - \frac{\tanh\left(\frac{\beta l_f}{2}\right)}{\frac{\beta l_f}{2}} \tag{2}$$

where β is the material parameter for steel fiber reinforced concrete, calculated as follows:

$$\beta = \sqrt{\frac{2\pi G_m}{E_f A_f \ln\left(\frac{S}{r_f}\right)}} \tag{3}$$

where G_m is the shear modulus of the matrix, E_f is the modulus of elasticity of the steel fibers, A_f is the fiber cross-sectional area, S is the spacing between the steel fibers and r_f is the equivalent radius of the steel fibers. In the respect the shear modulus of the matrix, G_m, is:

$$G_m = \frac{E_c}{2(1+v)} \tag{4}$$

where E_c is the modulus of elasticity of concrete and v is the Poisson's ratio of concrete.

The spacing between the steel fibers is:

$$S = 25\left(\frac{d_f}{\rho l_f}\right)^{0.5} \tag{5}$$

The bond efficiency factor, τ_b, was assumed as 1 in this research, while the interfacial bond stress between fiber and matrix, τ, was taken as 2.44 N/mm^2 (11). The tensile force in the tension zone of the section consists of the tensile force due to the prestressing strand, T1, force due to the deformed steel bar, T2, and the tensile force of fibrous reinforced concrete, T3, T4 and T5. The previous tensile forces are calculated as follows:

$$T_1 = A_{ps} f_{ps} \tag{6}$$

$$T_2 = A_s f_Y \tag{7}$$

where A_{ps} is the area of the prestressing strand, f_{ps} is the stress in the prestressing strand at ultimate load of the beam after considering all losses, A_s is the area of non-prestressed longitudinal tension reinforcement, and f_Y is the yield stress of the deformed bars.

$$T_3 = b(h - Z)\sigma_{cu} \tag{8}$$

$$T_4 = \frac{b}{2}(h - Z)(f_r - \sigma_{cu}) \tag{9}$$

$$T_5 = 0.5b\sigma_m(Z - c) \tag{10}$$

The compression force, C, consists of the force of concrete and the force of the compression steel, A'_S. In this research, the maximum strain of concrete, ϵ_c, at the extreme compression fiber was taken 0.003. The equilibrium equation of forces on the section are the same for partially and fully prestressed beams except that in fully prestressed beams, there is no tension force due to flexural steel bars, accordingly, the general form of the equation is as follows:

$$0.85 f'_c a(350) + A'_S = T_1 + T_2 + T_3 + T_4 + T_5 \tag{11}$$

There were two unknowns in Eq. (11); namely the stress in the prestressing strand after all losses, f_{ps}, and the distance from extreme compression fiber of the cross section to the neutral axis, C. The previous two values were obtained by trial and error. The nominal moment of the section was calculated after getting the values of the compression force and the tension forces. Afterward, the peak load was calculated according to the test setup used in this research.

Discussion of analytical results

Table 4 shows the comparison, between the experimental and analytical peak loads for the fully and the partially prestressed beams containing steel fibers. The table shows that the ratio between the analytical and experimental peak loads for fully and partially prestressed beams varied from 0.95 to 1. This clearly reveals the validity of the analytical model used in this study.

Table 4 also shows that the validated model also confirmed all the key test results and findings of this study. In fact, the analytical peak load of control beam B5-PP-0-0 of group two with PPR = 0.73 was higher than the control beam B1-FP-0-0 of group one with PPR = 1. In addition, the analytical peak loads of all beams of groups one and two containing steel fibers were higher than the respective control

Table 4 Comparisons between analytical and experimental peak loads.

Group	Beam	Peak load (experimental)	Peak load (analytical)	Ratio between experimental to analytical peak loads
One	B1-FP-0-0	67.28	66.7	1
	B2-FP-0.5-S	69.83	72.23	0.96
	B3-FP-1-S	72.2	73.1	0.98
	B4-FP-1.5-S	75	74.4	1
Two	B5-PP-0-0	71.85	68.1	1.05
	B6-PP-0.5-S	73.56	76	0.96
	B7-PP-1-S	74.8	78.25	0.95
	B8-PP-1.5-S	77.82	80	0.97

ones. Furthermore, the analytical peak loads increased by increasing the steel fibers' content. On the other hand, beam B8-PP-1.5-S of group two with PPR = 0.73 showed the highest analytical peak load when compared to all beams of groups one and two. Finally, the analytical model confirmed the previous finding that increasing the steel fibers' content increases the peak load of the beams.

Generally, the validated analytical model can be used with confidence to conduct future parametric studies aiming at establishing design oriented conclusions in the field.

Conclusions

An experimental and theoretical investigation on the behavior of fibrous post-tensioned concrete beams was conducted:

Adding steel fibers resulted in higher efficiency for fully and partially prestressed beams in terms of all aspects of structural behavior till failure.

The following enhancement in the behavior of fibrous post-tensioned concrete beams can be conducted:

1. Significant increase in the tensile strength of the concrete ranges from 2.6% to 29.7% and 1.2% to 29.5% for fully and partially prestressed beams respectively, decrease in the cracks widths and decrease in the spaces between cracks.
2. Increase in the flexural stiffness decrease the deflection and the tensile stress of the steel reinforcement.
3. Increase in peak load ranges from 3.78% to 11.48% and 2.38% to 8.32%, enhancement in ductility ranges from 7.2% to 26.22% and 13.39% to 27.63% and energy absorption ranges from 8.86% to 45.18% and 14.33% to 33.37% for fully and partially prestressed beams respectively.

Adding polypropylene fibers resulted in lower efficiency when compared to the steel fibers for partially prestressed beams in terms of all aspects of structural behavior till failure and resulted in the following advantages and disadvantages:

1. Decrease in the cracking load of the concrete ranges from −4.2% to −21.4% and the peak load ranges from −15% to −1.9%.
2. Only a slight increase of the flexural stiffness and a slight decrease of the cracks widths and the spacing between cracks was seen.
3. Only a slight decrease in the tensile steel stress of the steel reinforcement was seen, on the other hand a slight increase in the deflection, ductility ranges from 5.7% to 17.9%, and the energy absorption ranged from 3.4% to 11.85%.

It should be also noted that the steel fibers and the polypropylene fibers did not affect the beams pre-cracking behavior and the beams failure mode. The analytical model used for beams containing steel fibers, showed a very good agreement with the measured peak load with error ranges from 4% to 5%. The analytical model proved to be valid and can be used with confidence to conduct future parametric studies aiming at establishing design oriented conclusions in the field.

References

[1] ACI COMMITTEE 318. Building Code Requirements for Reinforced Concrete (ACI 318–08). American Concrete Institute, 2008.
[2] A.E. Naaman, S.M. Jeong, Structural ductility of concrete beams prestressed with FRP tendons, in: Proceeding of the Second International RILEM Symposium (FRPRCS-2), E& FN Spon, 1995, 379–401.
[3] R.N. Swamy, Sa'ad A. Al-Ta'an, Deformation and ultimate strength in flexure of reinforced concrete beams with steel fiber concrete, ACI Struct. J. 78 (5) (1981) 395–405.